18,12

Delamination of multilayer graphene nanoribbons on flat substrates

© A.V. Savin[1,2], A.P. Klinov[1]

[1] N.N. Semenov Federal Research Center for Chemical Physics, Russian Academy of Sciences, Moscow, Russia
[2] Plekhanov Russian University of Economics, Moscow, Russia

E-mail: asavin00@gmail.com, artemklinov@gmail.com

Received May 27, 2022
Revised June 13, 2022
Accepted June 14, 2022

Using molecular dynamics simulation, we have shown that multilayer graphene nanoribbons located on the flat surface of the h-BN crystal (on the flat substrate) delaminate due to thermal activation into a parquet of single-layer nanoribbons on the substrate. The delamination of graphene nanoribbons requires overcoming the energy barrier associated with the initial shift of its upper layer. After overcoming the barrier, the delamination proceeds spontaneously with the release of energy. The value of this barrier has been estimated and the delamination of two-layer nanofilms has been simulated. The existence of two delamination scenarios has been shown. The first scenario is the longitudinal (along the long side of the nanoribbon) sliding of the upper layer. The second one is in the sliding of the upper layer with the rotation of the layers relative to each other. The first scenario is common for elongated nanoribbons, the second — for two-layer graphene flakes having close to a square shape.

Keywords: graphene, multilayer nanoribbons, flat substrate, nanoribbon delamination.

DOI: 10.21883/PSS.2022.10.54252.390

1. Introduction

Layered two-dimensional (2D) materials such as graphene (G), hexagonal boron nitride (h-BN), molybdenum and tungsten disulfides (MoS_2, WS_2) attract great interest because of their unique electronic [1–3] and mechanical [4–7] properties. Currently, heterogeneous layered materials are of increased interest, which can demonstrate various new physical properties compared to their homogeneous analogues [8–10]. For example, the use of heterostructures G/h-BN makes it possible to obtain the necessary electronic properties [11,12], as well as significantly reduce friction between layers [13].

Graphene nanoribbons are ultra-soft on bending, they can slide over each other, bend, filling the irregularities of the substrate [7]. This allows multilayer nanoribbons placed on a flat substrate (for example, using the technique described in [7]), under mechanical stress on it, to delaminate and form a smooth „parquet“ on it from single-layer nanoribbons [14]. It was noted in the study [15] that ideal flat surfaces of multilayer crystals have the ability to self-purify from contaminants. This study will show that on the flat surface of a multilayer crystal, for example, on the surface of h-BN, multilayer graphene nanoribbons can, due to thermal activation, spontaneously delaminate, turning the rough surface initially contaminated with them into a perfectly smooth one. Using a coarse-grained 2D chain model and an all-atom 3D-model, the process of delamination of multilayer graphene nanoribbons on the surfaces of h-BN and graphite crystals will be simulated. The work is structured as follows. In Sec. 2 a 2D chain model is constructed, which is then used to simulate the displacement of layers of multilayer graphene nanoribbons. In Section 3 we simulate the delamination of multilayer graphene nanoribbons located on the flat surface of the h-BN crystal. In Section 4 we simulate the delamination of nanoribbons on a flat surface of a graphite crystal. In Section 5 we discuss the delamination of two-layer nanoribbons using a full-atomic 3D-model, analyze the influence of the shape of the nanoribbon on the rate of separation of its layers. Conclusion is presented in Section 6.

2. 2D-model

To describe the dynamics of layered structures from sheets and nanoribbons of graphene (G), hexagonal boron nitride (h-BN), it is convenient to use a two-dimensional model of the molecular chain system [16–18]. If we assume that the nanosheets (nanoribbons) G and h-BN lie in such a way that the zigzag direction of all of them coincides with the axis x (see Fig. 1), then the two-dimensional chain model will describe the cross section of the multilayer system along the axis x. Then one particle in the two-dimensional model will correspond to all the atoms of the nanoribbon that have the same coordinates x, z.

If atoms along the same line parallel to the y axis move synchronously, changing only the coordinates x, z, then the Hamiltonian of one graphene nanoribbon (h-BN) will have

the form of a Hamiltonian of chain located in plane xz:

$$H_i = \sum_{n=1}^{N} \left[\frac{1}{2} M_i(\dot{\mathbf{u}}_n, \dot{\mathbf{u}}_n) + V_i(R_n) + U_i(\theta_n) \right]. \qquad (1)$$

Here, the index $i = 1$ if the graphene nanoribbon (G) is considered, and $i = 2$ if the boron nitride nanoribbon (h-BN) is considered. Two-dimensional vector $\mathbf{u}_n = (x_n, z_n)$ sets the coordinates of the n-th particle of the chain. The particle mass for the G chain is the same as the mass of the carbon atom $M_1 = M_C = 12m_p$, and for the BN chain — it equals to the mean mass of boron and nitrogen atoms $M_2 = (M_B + M_N)/2 = 12.41m_p$ ($m_p = 1.66 \cdot 10^{-27}$ kg — the mass of the proton).

The potential

$$V_i(R) = \frac{1}{2} \kappa_i (R - R_i)^2 \qquad (2)$$

describes the longitudinal stiffness of the chain, κ_i — the stiffness of the interaction, R_i — the equilibrium length of the bond (chain pitch), $R_n = |\mathbf{u}_{n+1} - \mathbf{u}_n|$ — distance between neighboring nodes n and $n + 1$.

The potential

$$U_i(\theta) = \varepsilon_i [1 + \cos(\theta)] \qquad (3)$$

describes the bending stiffness of a chain, θ — angle between two adjacent bonds, $\cos(\theta_n) = -(\mathbf{v}_{n-1}, \mathbf{v}_n)/R_{n-1}R_n$, vector $\mathbf{v}_n = \mathbf{u}_{n+1} - \mathbf{u}_n$.

The parameters of the potentials (2), (3) for the G chain are defined in [16,17], and for the h-BN chain in [19] from the analysis of dispersion curves of graphene and boron nitride nanoribbons. For chain G longitudinal stiffness $\kappa_1 = 405$ N/m, chain pitch $R_1 = r_{CC}\sqrt{3}/2 = 1.228$ Å ($r_{CC} = 1.418$ Å — valence bond length C–C in graphene sheet), energy $\varepsilon_1 = 3.5$ eV. For the h-BN chain, the stiffness $\kappa_2 = 480$ N/m, pitch $R_2 = r_{\mathrm{BN}}\sqrt{3}/2 = 1.252$ Å ($r_{\mathrm{BN}} = 1.446$ Å — the length of the valence bond B–N in the sheet h-BN), energy $\varepsilon_2 = 1.10$ eV.

We note that the Hamiltonian of the chain (1) gives the deformation energy of the nanoribbon, which falls on the longitudinal band of the width $\Delta y = \sqrt{3} R_i$. Further, the energy of the chains will be normalized by the graphene nanoribbon, so the energy of the h-BN nanoribbons must be normalized by multiplying by $c = R_1/R_2 = r_{CC}/r_{\mathrm{BN}} = 0.9808$.

Pair interactions of chain nodes are described with high accuracy by Lennard–Jones potentials (5,11)

$$W_i(r) = \varepsilon_i \left[5(r_i/r)^{11} - 11(r_i/r)^5 \right]/6. \qquad (4)$$

Here r — the distance between the interacting nodes, ε_i — interaction energy, r_i — the equilibrium length (index $i = 1$ if the interaction of the nodes of the chain G is described, $i = 2$ — the interaction of the nodes of the h-BN chain, $i = 3$ — the interaction of the node of the G chain with the node of the h-BN chain). Potential parameters (4): $\varepsilon_1 = 0.00832$ eV, $r_1 = 3.607$ Å [20]; $\varepsilon_2 = 0.01511$ eV, $r_2 = 3.642$ Å; $\varepsilon_3 = 0.01433$ eV, $r_3 = 3.701$ Å [19].

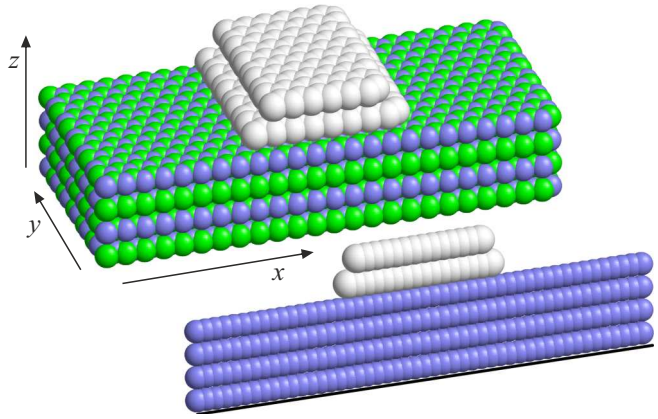

Figure 1. The scheme for constructing a two-dimensional chain model for a two-layer graphene flake lying on a flat surface of a h-BN crystal.

Number of layers should be limited when modeling the dynamics of a multilayer substrate. Therefore, we will assume that the first (lowest) layer interacts with a fixed flat surface of the crystal (on Fig. 1, this surface is shown by a black line). The interaction energy of the atoms of the layers with a fixed substrate can be described by the (k, l) Lennard–Jones potential

$$P_i(h) = e_i \left[k(h_i/h)^l - l(h_i/h)^k \right]/(l - k), \qquad (5)$$

where h — the distance of the atom to the plane of the fixed substrate, e_i — interaction energy, h_i — the equilibrium length, exponents are $l = 10$, $k = 3.75$. Index $i = 1$ for a multilayer sheet G, $i = 2$ — sheet BN. Potential parameters (5): $e_1 = 0.0903$ eV, $h_1 = 3.46$ Å [19]; $e_2 = 0.0974$ eV, $h_2 = 3.49$ Å [20].

Let us examine K-layer structures presented in Fig. 1. Let us assume, that the first $k = 1, \ldots, K_1$ layers correspond to BN chains (h-BN crystal layers), consisting from $N_k = N_{bn}$ links. These layers are on a flat fixed substrate and interact with it (let us assume, that fixed substrate surface coincides with $z = 0$ plane). The last K_2 layers ($K = K_1 + K_2$) correspond to the G chains of K_2-layered nanoribbon (flake) of graphene lying on the multilayer substrate h-BN. The coordinates of such a system of K chains are given by vectors

$$\left\{ \mathbf{u}_{n,k} = (x_{n,k}, z_{n,k}) \right\}_{n=1,k=1}^{N_k,K},$$

where n — the node number of the k-th chain (N_k — the number of nodes in the chain). The Hamiltonian of the chain system will have the form

$$H = \sum_{j=1}^{K_1} \sum_{n=1}^{N_{bn}} \frac{1}{2} cM_2(\dot{\mathbf{u}}_{n,j}, \dot{\mathbf{u}}_{n,j}) + \sum_{j=K_1+1}^{K} \sum_{n=1}^{N_j} \frac{1}{2} M_1(\dot{\mathbf{u}}_{n,j}, \dot{\mathbf{u}}_{n,j}) + E_1 + E_2 + E_3, \qquad (6)$$

where the potential energy of the G chain system

$$E_1 = \sum_{j=K_1+1}^{K} \sum_{n=1}^{N_j} [V_1(R_{n,j}) + U_1(\theta_{n,j})] + \sum_{i=K_1+1}^{K-1} \sum_{j=i+1}^{K} \sum_{n=1}^{N_i} \sum_{k=1}^{N_j} W_1(r_{n,i;k,j}), \quad (7)$$

energy of BN chain system

$$E_2 = c \sum_{j=1}^{K_1} \sum_{n=1}^{N_{bn}} [V_2(R_{n,j}) + U_2(\theta_{n,j}) + P_2(z_{n,j})] + c \sum_{i=1}^{K_1-1} \sum_{j=i+1}^{K_1} \sum_{n=1}^{N_{bn}} \sum_{k=1}^{N_{bn}} W_2(r_{n,i;k,j}), \quad (8)$$

interaction energy of G chains with BN chains

$$E_3 = \sum_{j=1}^{K_1} \sum_{i=K_1+1}^{K} \sum_{n=1}^{N_{bn}} \sum_{k=1}^{N_i} W_3(r_{n,j;k,i}). \quad (9)$$

3. Delamination of graphene flakes on substrate h-BN

Let us first analyze the process of delamination of a two-layer graphene flake located on the flat surface of the h-BN crystal — see Fig. 2, *a*. Let us assume that the substrate consists of three h-BN chains lying on a fixed substrate ($K_1 = 3$, $N_{bn} = 300$), and a two-layer G chain ($K_2 = 2$, $N_2 \le N_1 = 100$) on it lies. Let us first consider a symmetrical configuration in which the upper layer of the flake lies completely above the lower one.

To find the stationary state of the system, it is necessary to numerically solve the problem for a minimum of potential energy

$$E = E_1 + E_2 + E_3 \to \min : \ \mathbf{u}_{n,j}{}_{n=1,j=1}^{N_j,K}. \quad (10)$$

To obtain a stationary state of the flake with the shifted upper layer, one need to move the upper chain to the right and, when solving the problem (10), fix x of the coordinate of the left end of the lower chain and the right end of the upper one. Then, by successively shifting the upper chain and solving the problem (10), we will get the dependence of the energy of the system E on the amount of overlap of the layers of the flake, which is conveniently characterized by the distance between the projections on the axis x of the right edges of the flake $d = x_{K,N_2} - x_{K-1,N_1}$.

The characteristic shape of dependencies $E(d)$ is shown in Fig. 3. If the upper layer of the flake is much smaller than the lower layer, then its displacement to the edge of the flake does not change the energy of the system at first. The energy begins to grow noticeably at a distance

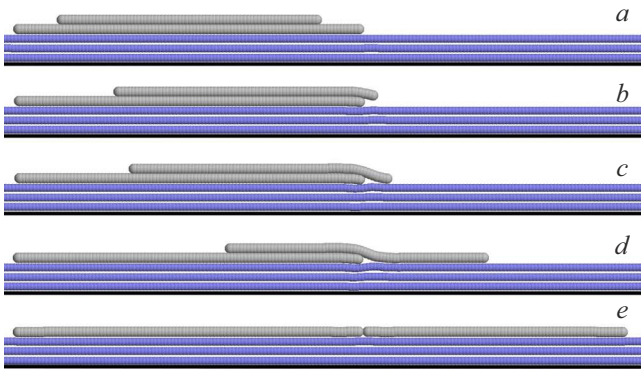

Figure 2. Change of the shape a two-layer graphene flake (number of links $N_1 = 100$, $N_2 = 75$) located on a multilayer substrate formed by the surface of the h-BN crystal from the distance d between projections on axis x of the right ends of the flake layers: (*a*) $d = -1.50$, (*b*) 0.47, (*c*) 0.98, (*d*) 4.48, (*e*) 9.43 nm.

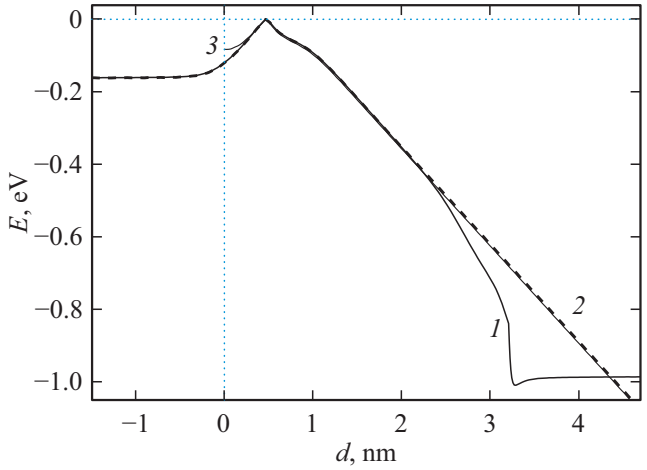

Figure 3. The dependence of the energy of a two-layer graphene flake E, located on a multilayer substrate formed by the surface of the h-BN crystal, from the distance d between the projections on the axis x of the right edges of the flake The number of links in the lower layer of the flake $N_1 = 100$, in the upper one — $N_2 = 25$, 75, 100 (curves *1, 2, 3*). Dependencies $E(d)$ are normalized so that the maximum energy value is zero.

between the edges of $d > -5$ Å and reaches a maximum value at $d = d_0 = 4.7$ Å. A further shift to the right leads to a monotonous decrease in energy. When $d = d_0$, the maximum allowable „cornice“ is formed, see Fig. 2, *b*. With further shift, the upper edge bends and touches the substrate (Fig. 2, *c*). Next, the upper layer slides onto the substrate (Fig. 2, *d*), the energy of the system decreases linearly with increasing displacement d. The minimum energy is achieved with the complete sliding of the upper layer from the lower one and the contact of their edges (Fig. 2, *e*). Further shifting of the upper layer of the flake leads to an increase in energy due to a decrease in the energy of the interaction of the edges. The interaction

energy of a carbon atom with an h-BN sheet is higher than the interaction energy with a graphene sheet. Therefore, it is always energetically more favorable for a graphene nanoribbon to lie on the surface of an h-BN crystal than to be on another graphene nanoribbon. To start sliding, the upper nanoribbon must go to the edge of the lower one and bend over it. This requires overcoming the energy barrier of $\Delta E = 0.16\,\text{eV}$ (if graphene nanoribbons have the same length, $\Delta E = 0.083\,\text{eV}$). After overcoming this barrier, further sliding of the upper layer will be accompanied by the release of energy. Note that this value of the barrier value is calculated per the band of the nanoribbon width $\Delta y = 3r_{CC}/2$. Therefore, the wider the two-layer nanoribbon, the greater the magnitude of the energy barrier of its delamination.

To describe the delamination scenario of a multilayer nanoribbon, consider a three-layer graphene nanoribbon located on the flat surface of the h-BN crystal, see Fig. 4, *a*. To find its ground state, it is necessary to numerically solve the problem for a minimum of (10) with $K_1 = 3$, $N_{bn} = 300$, $K_2 = 3$, $N_1 = N_2 = N_3 = N$. To obtain a stationary state of the flake with shifted layers, it is necessary to move the lower chain to the right and, when solving the problem (10), fix x of the coordinate of the right end of the lower chain and the left end of the second chain. Then, sequentially shifting the lower chain and solving the problem (10), we get the dependence of the energy of the system E from the amount of overlap of the first two layers of the flake, which is conveniently characterized by the distance between the projections on the axis x of the right ends of the first two layers of the flake $d = x_{K_1+1,N} - x_{K_1+2,N}$.

The characteristic shape of dependencies $E(d)$ is shown in Fig. 5. In the ground state, when all chains are located strictly above each other, the displacement of the lower chain $d = -0.1$ Å, see Fig. 4, *a*. Shifting to the right of the lower chain first leads to an increase in energy, which reaches its maximum value at $d = d_0 = 5.8$ Å (Fig. 4, *b*). Further displacement leads to a monotonous decrease in energy. At the $d = d_0$, the maximum allowable „cornice“ is formed from the two upper layers. With further displacement, the upper two-layer chain bends and comes into contact with the substrate (Fig. 4, *c*). Next, the upper layers slide onto the substrate (Fig. 4, *d*), the energy of the system decreases as a linear function d. The minimum energy is achieved with the complete detaching of the lower layer from under the upper layers and the contact of their edges — with the formation of two-layer and single-layer nanoribbons adjacent to each other (Fig. 4, *e*). Further displacement of the lower layer leads to an increase in energy due to a decrease in the interaction energy of the edges of these nanoribbons.

Thus, for the delamination of a three-layer nanoribbon, it is necessary to overcome the energy barrier $\Delta E = 0.10\,\text{eV}$, the value of which does not depend on the length of the nanoribbon. The same scenario of delamination with a shift along the substrate of the lower layer is realized for nanoribbons with a large number of layers. At $K_2 > 3$, a complete shift of the lower layer will require overcoming the barrier $\Delta E = 0.11\,\text{eV}$. We note that the delamination scenario of the nanoribbon with a slide to the substrate of its upper layer requires overcoming a higher energy barrier.

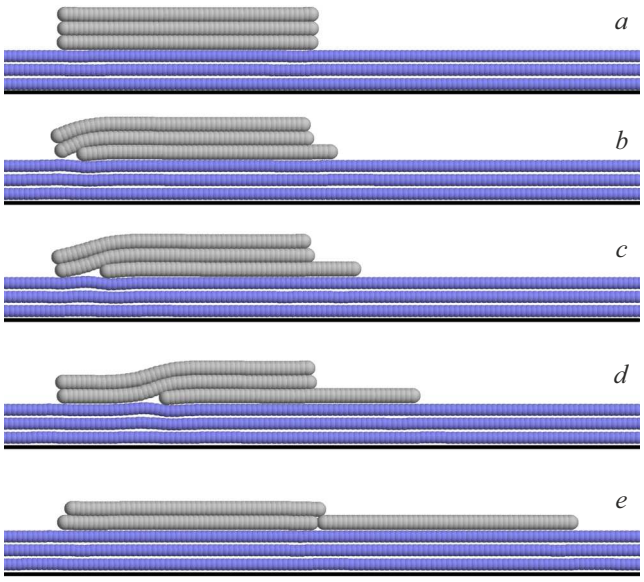

Figure 4. Change of the shape of a three-layer graphene nanoribbon (number of links $N_1 = N_2 = N_3 = 50$) located on a multilayer substrate formed by the surface of the h-BN crystal from the distance d between the projections on the axis x of the right edges of the first two layers of the nanoribbon: (*a*) $d = -0.01$, (*b*) 0.58, (*c*) 1.13, (*d*) 2.53, (*e*) 6.34 nm.

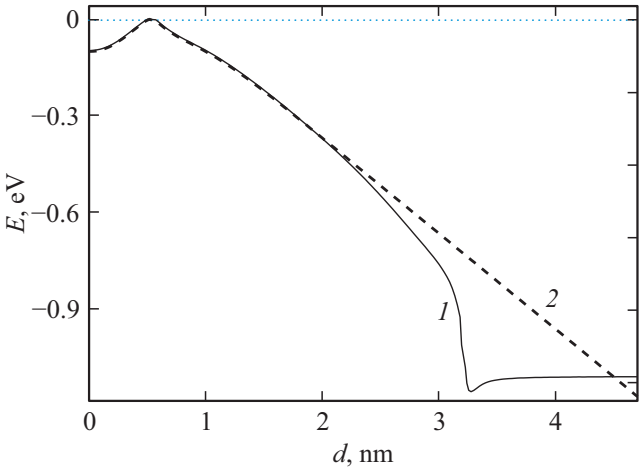

Figure 5. The dependence of the energy of a three-layer graphene nanoribbon E, located on a multilayer substrate formed by the surface of the h-BN crystal, on the distance d between projections on the axis x of the right edges of the first and second layers with the number of links $N_1 = N_2 = N_3 = 25$ and 50 (curves *1* and *2*). Dependencies $E(d)$ are normalized so that the maximum energy value is zero.

4. Delamination of graphene flakes on crystalline graphite substrate

Let us analyze the process of delamination of a two-layer graphene flake located on a flat surface of crystalline graphite, see Fig. 6, *a*. In this case, the interaction energy of the layers of the flake coincides with the energy of interaction with the layers of the substrate. Here, the energy gain from the delamination of the flake is associated with the ability to increase the energy of interaction of its edges.

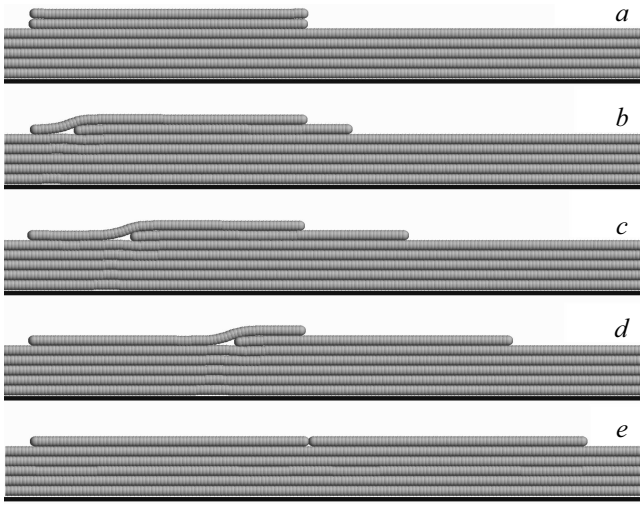

Figure 6. Change of the shape of a two-layer graphene flake (number of links $N_1 = N_2 = 75$) located on a multilayer substrate formed by the surface of crystalline graphite from the distance d between projections on the axis x of the right edges of the first two layers of the flake: (*a*) $d = -0.02$, (*b*) 1.52, (*c*) 3.52, (*d*) 7.02, (*e*) 9.43 nm.

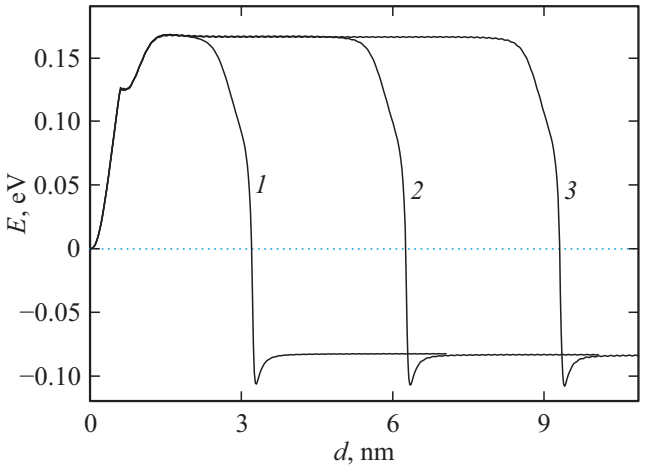

Figure 7. The dependence of the energy of a two-layer graphene nanoribbon E, located on a multilayer substrate formed by the surface of a graphite crystal, on the distance d between projections on the axis x of the right edges of the first and second layers with the number of links $N = 25$, 50 and 75 (curves *1, 2* and *3*). The dependences $E(d)$ are normalized so that the energy of the two-layer nanoribbon in the ground state is zero.

Let us assume that the substrate consists of $K_1 = 5$ G chains lying on a fixed substrate. Potential energy of the system of $K = K_1 + 2$ chains

$$E = \sum_{j=1}^{K}\sum_{n=1}^{N_j}[V_1(R_{n,j}) + U_1(\theta_{n,j}) + P_1(z_{n,j})] + \sum_{j=1}^{K-1}\sum_{j=i+1}^{K}\sum_{n=1}^{N_i}\sum_{k=1}^{N_j} W_1(r_{n,i;k,j}). \quad (11)$$

Let us take the number of links for the first five chains modeling a multilayer substrate $N_1 = \ldots = N_5 = 300$, and $N_6 = N_7 = N$.

The numerical solution of the problem for the minimum potential energy showed that the shift to the right of the lower chain of the two-layer nanoribbon first leads to an increase in energy, which reaches a maximum when shifting $d = 1.52$ nm, see Fig. 6, *b*. With this shift, the left edge of the top nanoribbon attaches to on the substrate. Further shifting of the lower nanoribbon does not result in a change in energy as long as the right edge of the upper nanoribbon remains lying above the lower (*c*), (*d*). The energy begins to decrease only when the right end of the upper nanoribbon slides off the lower one. The most energetically favorable state is obtained by the complete sliding of the end and the formation of two adjacent single-layer nanoribbons (*e*).

Dependence of the energy of a two-layer nanoribbon E on the magnitude of the shift of their layers d is shown in Fig. 7. The delamination of the nanoribbon requires overcoming the energy barrier $\Delta E_0 = 0.168$ eV. The magnitude of this barrier does not depend on the length of the nanoribbon (it corresponds to the bending energy of a single-layer nanoribbon when it is raised from the substrate to the edge of another layer). The width of the barrier corresponds to the length of the nanoribbon. The energy gain from the delamination of the nanoribbon $\Delta E_1 = 0.11$ eV also does not depend on the length of the nanoribbon.

5. 3D-model

The use of a chain 2D-model allows one only to qualitatively describe the mechanisms of delamination of multilayer nanoribbons. A more detailed description necessitates the use of 3D-models requiring much larger computational resources for numerical modeling. Therefore, we will confine ourselves here only to modeling the delamination of two-layer graphene nanoribbons located on a fixed flat substrate that serves as a model of the surface of the h-BN crystal.

The Hamiltonian of a two-layer graphene nanoribbon, each layer of which consists of N atoms, located on a flat

substrate, has the appearance

$$H = \sum_{i=1}^{2}\sum_{n=1}^{N}\left[\frac{1}{2}M_{n,i}(\dot{\mathbf{u}}_{n,i},\dot{\mathbf{u}}_{n,i}) + E_{n,i} + P(z_{n,i})\right] + \sum_{n=1}^{N}\sum_{k=1}^{N}W(r_{n,1;k,2}), \quad (12)$$

where the vector $\mathbf{u}_{n,i} = (x_{n,i}, y_{n,i}, z_{n,i})$ specifies the coordinates of the n-th carbon atom of the i-th nanoribbon ($i = 1, 2$).

The first term of the sum (12) specifies the kinetic energy. Let us assume that hydrogen atoms are attached to the edge atoms of nanoribbons, so the mass of the inner atoms $M_{n,i} = 12m_p$, and the $M_{n,i} = 13m_p$ (m_p — the mass of the proton). The term $E_{n,i}$ sets the interaction energy of the n-atom of the i-of that nanoribbon with neighboring nanoribbon atoms (the deformation of valence bonds, valence and torsion angles, as well as paired interactions of atoms are taken into account — a detailed description of the used force the fields are given in [21]). The $P(z)$ potential describes the interaction energy of a nanoribbon atom with a flat substrate (5) where the interaction energy $e_1 = 0.0903$ eV and the equilibrium distance $h_1 = 3.46$ Å.

The last term in the formula (12) describes the energy of the van der Waals interaction of atoms of different nanoribbons, $r_{n,1;k,2} = |\mathbf{u}_{k,2} - \mathbf{u}_{n,1}|$ — the distance between the n-th atom of the first and k-th atom of the second nanoribbon, potential

$$W(r) = \varepsilon_c[(r_c/r)^6 - 1]^2 - 1, \quad (13)$$

where $\varepsilon_c = 0.002757$ eV, $r_c = 3.807$ Å.

Let us first take the ground state of a two-layer nanoribbon located on a flat h-BN substrate. To do this, we will numerically solve the problem for a minimum of potential energy

$$E = \sum_{i=1}^{2}\sum_{n=1}^{N}[E_{n,i} + P(z_{n,i})] + \sum_{n=1}^{N}\sum_{k=1}^{N}W(r_{n,1;k,2}) \to \min: \ \mathbf{u}_{n,i}{}_{n=1,i=1}^{N,2}. \quad (14)$$

Then we put the nanoribbon in a Langevin thermostat and get its thermalized state. For this purpose, let us numerically integrate the system of Langevin equations

$$M_{n,i}\ddot{\mathbf{u}}_{n,i} = -\frac{\partial H}{\partial \mathbf{u}_{n,i}} - \Gamma M_{n,i}\dot{\mathbf{u}}_{n,i} + \Xi_{n,i}, \quad (15)$$

$$n = 1, \ldots, N, \quad i = 1, 2,$$

with an initial condition corresponding to the ground state of a two-layer nanoribbon. Here $\Gamma = 1/t_r$ — coefficient of friction characterizing the intensity of energy exchange with the thermostat (relaxation time $t_r = 0.2$ ps), $\Xi_{n,i} = \{\xi_{n,i,j}\}_{j=1}^{3}$ — three-dimensional vector of normally distributed random forces normalized by conditions

$$\langle \xi_{n,i_1,j_1}(t_1)\xi_{k,i_2,j_2}(t_2)\rangle = 2M_{n,i_1}k_{\mathrm{B}}T\delta_{nk}\delta_{i_1i_2}\delta_{j_1j_2}\delta(t_2 - t_1)$$

(T — thermostat temperature, k_{B} — Boltzmann constant).

During the $t = 10t_r$, the two-layer nanoribbon reaches a thermalized state with a temperature T. Next, we turn off the interactions with the thermostat by removing the last two terms in (15) and analyze further dynamics of the system. The dynamics will be analyzed according to 256 trajectories corresponding to independent realizations of the initial thermalized state.

We used LAMMPS program for our numerical simulations [22]. Pair interactions are described by the Lennard–Jones potential (13) with cutoff radius $r_s = 20$ Å smoothed to zero in the range 19−20Å.

For certainty, let us take a two-layer nanoribbon consisting of layers of the same size, with a zigzag structure along the axis x, see Fig. 1. Consider a nanoribbon with a width of $L_y = 1.1$ nm and a length of $L_x = 5.9,\ 12.0,\ 24.3$ nm (the number of atoms in one layer of the nanoribbon $N = 294,\ 594,\ 1194$). Modeling the shift of the upper layer of the nanoribbon along the axis x showed that the upper layer forms the largest cornice when it is shifted by 5−6 Å, the further shift leads to the bending over of the upper layer and its adhesion to the substrate. To start the delamination of the nanoribbon, it is necessary to overcome the energy barrier of height $\Delta E = 0.081$ eV to the width of $\Delta y = 3r_{CC}/2$. This value is in good agreement with the result of $\Delta E = 0.083$ eV obtained when using a 2D chain model.

The delamination of the nanoribbon requires a thermally activated overcoming of a sufficiently high barrier. Therefore, during the possible time of numerical simulation on modern supercomputers, it is possible to simulate the delamination only at high temperatures $T \geq 900$ K.

Modeling showed that two delamination scenarios are possible. The first scenario is the longitudinal (along the long side) displacement of the layers, see Fig. 8, *a*. This delamination mechanism is well described by the 2D-model. In the second scenario detaching of layers is accompanied by their relative rotation. After the initial rotation, the upper layer slides over the long edge of the lower one, see Fig. 8, *b*. The first scenario is common for elongated nanoribbons with an aspect ratio of 3 : 1 and more, and the second — for two-layer flakes having close to the square shape.

Analysis of the dependence of the delamination time (the time during which the complete detaching of layers occurs) on the temperature value showed that the elongated nanoribbons are most rapidly exfoliated, see Fig. 9. For all nanoribbons, the time of their delamination is proportional to the exponent of the inverse temperature

$$t_d \approx c_2 \exp(c_1 T^{-1}), \quad (16)$$

where the coefficients c_1 and c_2 depend on the size and shape of the nanoribbon (on its aspect ratio). The

resulting approximation (16) allows one to make estimates of the value of the delamination time at $T = 300\,\mathrm{K}$. So for nanoribbons of size 5.9×1.1, 24.3×1.1, 12.0×1.1 and $7.1 \times 2.0\,\mathrm{nm}^2$ their delamination time is $t_d \approx 0.2$, 22, 0.15 10^{-4} s and 0.3 s, respectively.

The exponential type of dependence of the delamination time on the inverse temperature (16) is explained by the need to overcome the energy barrier during the initial separation of the layers, the magnitude of which is proportional to the width of the edge along which the delamination occurs. We note that at high temperatures, the discreteness of nanoribbons has practically no effect on their dynamics. The effects of discrete structure resulting in static friction [23] will occur only at low temperatures $T < 100\,\mathrm{K}$.

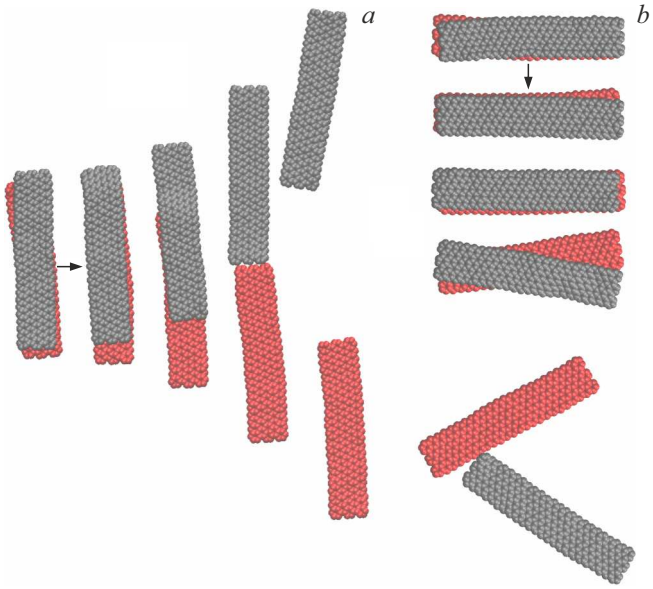

Figure 8. Longitudinal (a) and transverse (b) delamination of a two-layer nanoribbon of size $L_x \times L_y = 5.9 \times 1.1\,\mathrm{nm}^2$. Red indicates the lower layer of the nanoribbon, gray — the upper one. The frames presented in the figure are taken from a numerical experiment at $T = 900\,\mathrm{K}$ with an interval of 5 ps (the arrows indicate the direction of the frames).

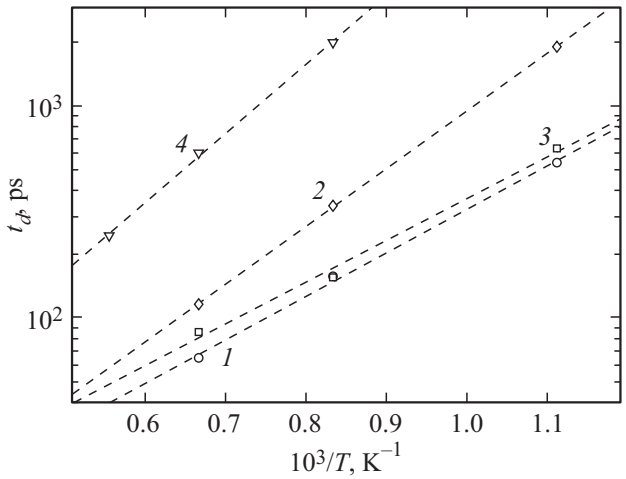

Figure 9. The dependence of the delamination time t_d on the reverse temperature T^{-1} for a two-layer graphene nanoribbon of size 5.9×1.1, $24.3 \times 1.1\,\mathrm{nm}^2$, 12.0×1.1 and $7.1 \times 2.0\,\mathrm{nm}^2$ (curves *1, 2, 3* and *4*). Dotted lines give dependencies $t_d = c_2 \exp(c_1 T^{-1})$. For curves *1, 2, 3* and *4*: $c_1 = 4734$, 6280, 4539 and 7522 K, $c_2 = 2.87$, 1.78, 3.92 and 3.83 ps, respectively.

For long nanoribbons, the delamination will occur according to the first scenario through its transverse (narrow) edge, see Fig. 8, *a*. The narrower the nanoribbon, the faster its delamination will occur. For graphene nanoflakes having close to the square shape, a second delamination scenario will be more probable. Here, it is energetically more advantageous to first rotate the layers relative to each other so that hanging corners form at the upper layer that directly interact with the substrate, and then the upper layer slides in the direction of these angles, see Fig. 8, *b*. The delamination of nanoribbons can be accelerated by mechanical action on the substrate.

6. Conclusion

The simulation shows that on the flat surface of a multilayer crystal, for example, on the surface of h-BN, multilayer graphene nanoribbons can spontaneously delaminate due to thermal activation, turning the rough surface initially contaminated with them into a perfectly smooth one. The delamination of a multilayered nanoribbon requires overcoming the energy barrier associated with the initial shift of its upper layers. After overcoming the barrier, the delamination already goes with the release of energy. The magnitude of this barrier is estimated. The consequence of the presence of a barrier is a directly proportional dependence of the delamination time of the nanoribbon on the exponent of the inverse temperature. Delamination of two-layer nanoribbons can occur in two scenarios. In the first scenario, the upper layer will slide from the lower along the edge of the nanoribbon, in the second — the sliding is accompanied by the rotation of the layers relative to each other. Modeling shows that for long nanoribbons, their delamination occurs according to the first scenario, and for short, close to the square shape — according to the second.

Funding

The research work was funded by subsidy allocated by the N.N. Semenov Federal Research Center for Chemical Physics of Russian Academy of Sciences (task No. FFZE-2022-0009) and by the Russian Foundation for Basic Research (project No. 20-33-90165). The calculations were carried out in Joint Supercomputer Center of Russian Academy of Sciences.

Conflict of interest

The authors declare that they have no conflict of interest.

References

[1] K.S. Novoselov, A.K. Geim, S.V. Morozov, D. Jiang, Y. Zhang, S.V. Dubonos, I.V. Grigorieva, A.A. Firsov. Science **306**, *5696*, 666 (2004).
[2] A.H. Castro Neto, F. Guinea, N.M.R. Peres, K.S. Novoselov, A.K. Geim. Rev. Mod. Phys. **81**, 109 (2009).
[3] E. Koren, I. Leven, E. Lörtscher, A. Knoll, O. Hod, U. Duerig. Nature Nanotech. **11**, 752 (2016).
[4] J.C. Meyer, A.K. Geim, M. Katsnelson, K. Novoselov, T. Booth, S. Roth. Nature **446**, 60 (2007).
[5] C. Lee, X. Wei, J.W. Kysar, J. Hone. Science **321**, 385 (2008).
[6] A. Falin, Q. Cai, E.J.G. Santos, D. Scullion, D. Qian, R. Zhang, Z. Yang, S. Huang, K. Watanabe, T. Taniguchi, M.R. Barnett, Y. Chen, R.S. Ruoff, L.H. Li. Nature Commun. **8**, 15815 (2017).
[7] E. Han, J. Yu, E. Annevelink, J. Son, D.A. Kang, K. Watanabe, T. Taniguchi, E. Ertekin, P.Y. Huang, A.M. van der Zande. Nature Mater. **19**, 305 (2020).
[8] I. Leven, D. Krepel, O. Shemesh, O. Hod. J. Phys. Chem. Lett. **4**, 115 (2013).
[9] A. Geim, I. Grigorieva. Nature **499**, 419 (2013).
[10] K.S. Novoselov, A. Mishchenko, A. Carvalho, A. H. Castro Neto. Science **353**, *6298*, 461 (2016).
[11] C.R. Woods, L. Britnell, A. Eckmann, R.S. Ma, J.C. Lu, H.M. Guo, X. Lin, G.L. Yu, Y. Cao, R.V. Gorbachev, A.V. Kretinin, J. Park, L.A. Ponomarenko, M.I. Katsnelson, Y.N. Gornostyrev, K. Watanabe, T. Taniguchi, C. Casiraghi, H.J. Gao, A.K. Geim, K.S. Novoselov. Nature Phys. **10**, 451 (2014).
[12] G.J. Slotman, M.M. van Wijk, P.L. Zhao, A. Fasolino, M.I. Katsnelson, S. Yuan. Phys. Rev. Lett. **115**, 186801 (2015).
[13] D. Mandelli, I. Leven, O. Hod, M. Urbakh. Sci. Rep. **7**, *1*, 10851 (2017).
[14] H.A. Loh, C. Marchi, L. Magagnin, K.A. Sierros. ACS Omega **6**, 30607 (2021).
[15] A.K. Geim. Nano Lett. **21**, 6356 (2021).
[16] A.V. Savin, E.A. Korznikova, S.V. Dmitriev. Phys. Rev. B **92**, 035412 (2015).
[17] A.V. Savin, E.A. Korznikova, S.V. Dmitriev. FTT **57**, *11*, 2278 (2015) (in Russian).
[18] A.V. Savin, E.A. Korznikova, S.V. Dmitriev. Phys. Rev. B **99**, 235411 (2019).
[19] A.V. Savin. ZhETF **160**, *6(12)*, 885 (2021) (in Russian).
[20] A.V. Savin, E.A. Korznikova, S.V. Dmitriev. Phys. Rev. B **99**, 235411 (2019).
[21] A.V. Savin, Yu.S. Kivshar, B. Hu. Phys. Rev. B **82**, 195422 (2010).
[22] S. Plimpton. J. Comput. Phys. **117**, 1 (1995).
[23] W. Ouyang, D. Mandelli, M. Urbakh, O. Hod. Nano Lett. **18**, *9*, 6009 (2018).